SUPPORTING INFORMATION - The evolution of thecideide microstructures and textures: traced from Triassic to Holocene

MARIA SIMONET RODA, ERIKA GRIESSHABER, LUCIA ANGIOLINI, DAVID A.T. HARPER, ULRICH JANSEN, MARIA ALEKSANDRA BITNER, DANIELA HENKEL, ELOY MANZANERO, TAMÁS MÜLLER, ADAM TOMAŠOVÝCH, ANTON EISENHAUER, ANDREAS ZIEGLER AND WOLFGANG W. SCHMAHL

Thecideide brachiopods are an anomalous group of invertebrates. In this study we discuss the evolution of thecideide brachiopods from the Triassic to Holocene and base our results and conclusions on microstructure and texture measurements gained from electron backscatter diffraction (EBSD). In fossil and Recent thecideide shells, we observe the following mineral units: (i) nanometric to small granules, (ii) acicles, (iii) fibres, (iv) polygonal crystals, (v) large roundish crystals. We trace for thecideide shells the change of mineral unit characteristics such as morphology, size, orientation, arrangement and distribution pattern. Triassic thecideide shells contain extensive sections formed of fibres interspersed with large, roundish crystals. Upper Cretaceous to Pleistocene thecideide hard tissues consist of a matrix of minute to small grains reinforced by acicles and small polygonal crystals. Recent thecideide species form their shell of mineral units that show a wide range of shapes, sizes and arrangements. We find from Late Triassic to Recent a gradual decrease in mineral unit size, regularity of mineral unit morphology and orientation, as well as calcite co-orientation strength. While crystallite co-orientation strength is the highest for fibrous microstructures, it is strikingly low for taxa that form their shell out of nanogranular to acicular mineral units. Our results indicate that Upper Jurassic species represent transitional forms between ancient taxa with fibrous shells and Recent forms that construct their shells of acicles and granules. We attribute the observed changes in microstructure and texture to be an adaptation to a different habitat and life-style associated with cementation to hard substrates.

Keywords: Brachiopoda, shell microstructure evolution, thecideides, calcite crystals, calcite fibre, EBSD

*Maria Simonet Roda * [simonet@lrz.uni-muenchen.de], Erika Griesshaber [e.griesshaber@lrz.uni-muenchen.de], Wolfgang W. Schmahl [*Wolfgang.W.Schmahl@lrz.uni-muenchen.de*], Department of Earth and Environmental Sciences, LMU München, 80333 Munich, Germany; Lucia Angiolini [*lucia.angiolini@unimi.it*], Dipartimento di Scienze della Terra "A. Desio", Università degli Studi di Milano, 20133 Milano, Italy; David A.T. Harper [*david.harper@durham.ac.uk*], Department of Earth Sciences, Durham University, Durham DH1 3LE, United Kingdom; Ulrich Jansen [*ulrich.jansen@senckenberg.de*], Senckenberg Forschungsinstitut und Naturkundemuseum Frankfurt, 60325 Frankfurt am Main, Germany; Maria Aleksandra Bitner [*bitner@twarda.pan.pl*], Institute of Paleobiology, Polish Academy of Sciences, 00-818 Warsaw, Poland; Daniela Henkel [*dhenkel@geomar.de*], Anton Eisenhauer [*aeisenhauer@geomar.de*], GEOMAR-Helmholtz Centre for Ocean Research, 24148 Kiel, Germany; Eloy Manzanero [*manzanero.paleoart@gmail.com*], Universidad Nacional de Educación a Distancia, UNED 28040 Madrid, Spain; Tamás Müller [*beregond02@gmail.com*], Adam Tomašových [*Adam.Tomasovych@savba.sk*], Earth Science Institute, Slovak Academy of Sciences, 974 01 Banská Bystrica, Slovakia; Andreas Ziegler [*andreas.ziegler@uni-ulm.de*], Central Facility for Electron Microscopy, University of Ulm, 89081 Ulm, Germany.*

Table S1 Sample numbers for the illustrated material.

Species	Age	Original location	Number	Repository
Thecospira tenuistriata Bittner, 1890	Late Triassic	Alpe di Specie, Italy	MPU5784-4 MPU5804	Museo di Paleontologia Dipartimento di Scienze della Terra Università degli Studi di Milano
Thecospira tyrolensis (Loretz, 1875)	Late Triassic	Alpe di Specie, Italy	MPU5484-4	Museo di Paleontologia Dipartimento di Scienze della Terra Università degli Studi di Milano
Bactrynium bicarinatum (Emmrich, 1855)	Late Triassic	Elberg Austria	E100-18-17	Ludwig Maximilian University of Munich
Neothecidella ulmensis (Quenstedt, 1858)	Late Jurassic (middle Oxfordian)	Bałtów, Poland	LMU-NU01	Ludwig Maximilian University of Munich
Thecidiopsis digitata (Sowerby, 1823)	Late Cretaceous	Petersberg, Maastricht, Netherlands	LMU-TD01	Ludwig Maximilian University of Munich
Thecidea papillata (Schlotheim, 1813)	Late Cretaceous	Symphorien, Mons, Belgium	LMU-TPLC01	Ludwig Maximilian University of Munich
Thecidea papillata (Schlotheim, 1813)	Paleocene	Ciply near Mons, Belgium	LMU-TPP01	Ludwig Maximilian University of Munich
Lacazella mediterranea (Risso, 1826)	Late Eocene	Dnipropetrovs k, Ukraine	LMU-LME01	Ludwig Maximilian University of Munich
Lacazella mediterranea (Risso, 1826)	Late Oligocene	Peyrere Aquitaine Basin, France	LMU-LMO01	Ludwig Maximilian University of Munich
***Thecidellina* sp.**	Pleistocene	Curaçao, Caribbean	UF 325201	Ludwig Maximilian University of Munich
Pajaudina atlantica Logan, 1988	Recent	Palma, Canary Islands, Spain	LMU-PA008 LMU-PA009 LMU-PA010 LMU-PA011	Ludwig Maximilian University of Munich

Table S2. The character matrix and taxa used for construction of the phylogenetic tree (see also Figure 13), based on the characters and character states described by Jaecks & Carlson (2001) with the addition of microstructure and texture results obtained in this study and the inclusion of the thecideide species *Neothecidella ulmensis*. Character numbers referring to microstructure and texture and character states are as follows:

38. Dorsal valve, extent of fibrous layer. 0 = covers entire valve; 1 = partial coverage; 2 = partial coverage, limited to sockets and/ or cardinal process; 3 = absent.

39. Ventral valve, extent of fibrous layer. 0 = covers entire valve; 1 = partial coverage; 2 = partial coverage, teeth only; 3 = absent.

40. Dorsal valve granular calcite. 0 = absent; 1 = present.

41. Ventral valve granular calcite. 0 = absent; 1 = present.

42. Dorsal valve acicular calcite. 0 = absent; 1 = present.

43. Ventral valve acicular calcite. 0 = absent; 1 = present.

50. Secondary fabric type. 0 = non-fibrous; 1 = fibrous

	1	2	3	4	5	6	7	8	9	10	11	12	13	14	15	16	17	18	19	20	21	22	23	24	25	26	27	28	29	30
Dielasma	1	0	2	?	?	0	1	0	?	0	0	1	0	1	1	0	0	0	0	0	0	0	0	0	0	?	2	0	?	?
Backhausina schluteri	0	3	3	1	?	0	0	3	0	3	2	2	1	1	1	2	0	2	?	0	0	?	?	?	1	3	2	2	1	2
Agerinella	0	3	5	1	?	0	0	3	1	0	0	?	0	?	?	2	?	?	?	?	?	?	?	?	1	?	2	?	1	0
Bactrynium bicarnatum	0	1	2	?	1	0	0	?	?	?	?	1	0	0	0	0	?	?	1	?	?	1	?	?	?	1	4	2	?	1
Bifolium faringdonense	0	0	4	1	3	0	0	3	0	2	3	1	0	1	0	1	1	1	2	1	1	0	0	1	1	1	2	2	2	0
Bitternella	0	3	?	1	1	0	0	?	?	?	3	0	0	1	1	1	1	1	?	?	?	?	?	?	1	?	2	?	1	1
Bosquetella campichei	0	0	0	2	1	0	0	0	?	0	0	0	0	1	?	?	?	1	?	3	2	?	?	?	1	1	2	0	2	0
Danella recurvirostris	0	1	0	2	1	0	0	0	?	2	3	1	0	?	?	2	1	2	2	3	1	1	?	?	1	2	2	1	1	2
Davidsoniella sinuata	0	1	5	2	1	0	0	?	1	2	3	2	0	0	0	1	2	1	2	2	?	2	?	1	0	2	2	0	1	0
Eothecidellina imperfecta	0	3	4	1	2	0	0	?	1	4	2	1	0	1	?	1	1	1	1	?	?	2	?	?	1	3	2	0	1	0
Eudesella mayensis	0	0	3	1	3	0	0	3	0	2	3	0	0	0	0	1	1	0	2	1	2	0	0	0	1	2	1	?	1	0
Glazewvskia	0	4	1	1	2	0	0	3	0	2	3	0	0	1	1	1	2	1	2	1	1	?	?	?	1	1	2	?	1	1
Konstantia	0	3	3	?	?	0	0	?	0	0	0	?	0	?	?	?	?	?	?	?	?	?	?	?	1	?	2	?	1	1
Lacazella	0	0	0	3	3	0	0	3	0	3	3	2	0	1	1	1	2	2	2	3	?	0	0	2	1	4	2	2	1	2

Mimikonstantia sculpta	0	3	3	1	2	0	0	?	1	1	1	1	0	0	0	2	2	1	0	1	?	4	?	1	1	1	?	0	1	0
Moorellina granulosa	0	3	0	3	3	0	0	3	0	0	0	2	0	1	1	1	1	0	2	?	?	0	0	1	1	4	2	?	2	0
Neothecidella ulmenensis	1	0	6	1	?	0	0	1	1	3	1	1	0	1	1	1	?	0	0	2	1	?	?	?	1	1	1	1	1	0
Neothecidella parviserrata	0	0	4	1	?	0	0	1	0	2	2	2	0	?	?	1	2	2	2	2	?	0	0	?	1	4	1	1	1	0
Pachymoorellina dundriensis	0	1	1	3	3	0	0	2	0	4	3	2	0	1	1	0	1	1	1	3	2	1	?	1	1	1	2	0	1	0
Pajaudina atlantica	0	3	3	1	2	0	0	3	0	3	3	2	0	1	1	1	1	1	2	2	2	0	0	2	1	2	1	2	1	2
Pamirotheca	0	1	2	2	1	0	0	?	?	?	1	?	0	1	1	?	?	1	?	?	?	?	?	?	1	?	?	0	1	0
Parabifolium	0	0	4	1	?	0	0	1	0	2	2	2	0	?	?	?	?	?	?	?	?	?	?	?	1	4	2	?	1	2
Parathecidea hieroglyphica	0	3	3	2	1	0	0	3	0	2	3	2	0	1	1	2	1	1	2	3	2	0	0	0	1	3	2	2	1	1
Praelacazella wetherelli	0	4	4	1	2	0	0	3	0	2	3	0	0	?	?	2	1	2	2	2	2	0	0	2	1	3	2	2	1	2
Rioultina ornata	0	3	0	2	1	0	0	3	0	2	2	2	0	1	1	2	1	1	?	2	1	?	?	?	1	1	?	0	1	0
Thecidea radiata	0	0	0	0	0	0	0	3	0	2	2	2	1	1	1	1	1	1	2	3	2	0	0	3	0	2	2	2	1	1
Thecidella rustica	0	3	5	1	3	0	0	0	?	0	0	0	0	1	?	3	1	0	0	2	?	2	?	1	1	3	2	0	1	0
Thecidellina congregata	0	0	1	3	3	0	0	3	0	2	2	1	0	1	?	1	1	1	0	2	1	2	2	?	1	1	2	2	1	0
Thecidiopsis digitata	0	3	3	3	3	0	0	3	0	2	3	2	0	?	?	1	1	1	2	3	2	0	0	3	1	3	2	2	1	1
Thecospira haidingeri	0	3	3	2	1	?	0	2	0	4	?	1	0	1	?	0	0	2	0	?	?	?	?	?	1	3	?	0	0	0
Hungaritheca	0	0	2	1	?	0	0	?	?	?	?	0	1	1	1	?	?	1	0	?	?	?	?	?	1	1	2	?	1	0
Thecospirella	0	3	2	1	?	0	0	?	?	?	3	0	1	1	1	1	1	1	?	?	?	?	?	?	1	?	2	?	1	0
Vermiculothecidea vermicularis	0	3	0	2	1	0	0	3	0	2	3	2	0	?	?	?	1	1	?	1	2	?	?	?	1	3	2	1	1	2
Eolacazella longirostrea	0	3	0	2	?	0	0	?	?	2	?	2	0	0	0	4	1	1	2	3	2	0	0	2	1	3	?	0	1	2
Stentorina sagittata	0	4	3	1	2	0	0	1	1	4	2	0	0	?	?	2	2	2	1	2	?	?	?	?	1	4	2	1	1	0
Ancorellina	0	4	1	2	2	0	0	2	1	?	?	0	0	2	0	2	0	2	0	?	?	?	?	?	1	3	2	?	1	?

Table S2 continued. The used matrix and taxa for construction of the phylogenetic tree (see also Figure 13).

	31	32	33	34	35	36	37	38	39	40	41	42	43	44	45	46	47	48	49	50	51	52	53	54
Dielasma	?	?	?	?	0	1	?	0	0	0	0	0	0	0	0	2	0	?	0	1	0	?	?	?
Backhausina schluteri	0	?	?	3	0	0	1	?	?	?	?	?	?	0	3	0	1	0	1	1	?	?	?	1
Agerinella	0	0	0	?	?	1	?	?	?	?	?	?	?	0	3	0	?	0	1	1	?	?	?	?
Bactrynium bicarnatum	0	0	0	1	0	1	?	0	0	0	0	0	0	0	4	0	1	0	1	1	2	0	?	0
Bifolium faringdonense	0	0	0	2	0	0	0	2	2	0	0	1	1	0	1	0	1	0	1	1	1	0	1	0
Bitternella	0	0	0	1	?	0	?	?	2	0	0	?	?	0	?	0	1	0	1	1	?	?	?	?
Bosquetella campichei	0	0	0	1	0	0	0	2	0	0	1	1	0	0	1	0	1	0	1	1	1	?	?	0
Danella recurvirostris	2	0	0	3	0	0	1	?	?	?	?	?	?	0	3	0	1	0	1	1	2	0	1	1
Davidsoniella sinuata	0	0	0	2	0	1	0	0	0	0	0	0	0	0	4	0	1	0	1	1	2	0	5	0
Eothecidellina imperfecta	0	0	0	2	0	0	0	2	0	0	0	0	0	0	1	0	1	0	1	1	1	0	1	0
Eudesella mayensis	0	?	?	0	1	0	0	0	0	0	0	0	0	0	4	0	0	0	1	1	1	?	0	0
Glazewvskia	0	?	?	3	0	0	?	?	?	?	?	?	?	0	3	0	1	0	1	1	?	?	?	0
Konstantia	0	1	0	0	1	?	?	?	?	?	?	?	?	0	1	0	1	0	1	1	1	0	0	?
Lacazella	2	0	0	3	0	0	1	2	2	1	1	1	1	0	3	0	1	0	1	0	2	1	1	0
Mimikonstantia sculpta	0	1	0	0	0	0	0	0	0	1	1	0	0	0	1	0	2	0	1	1	1	?	0	0
Moorellina granulosa	0	0	0	5	0	0	0	0	0	0	0	0	0	0	1	0	1	0	1	1	1	?	?	0
Neothecidella ulmenensis	0	0	0	1	0	0	0	0	2	0	0	1	1	0	3	0	1	0	1	1	2	0	5	?
Neothecidella parviserrata	0	0	0	1	0	0	0	2	2	0	0	1	1	0	3	0	1	0	1	1	2	0	5	?
Pachymoorellina dundriensis	0	0	0	0	1	0	0	1	1	0	0	0	1	0	1	0	1	0	1	0	1	0	0	0
Pajaudina atlantica	2	0	0	3	0	1	1	2	2	1	1	1	1	0	3	0	1	0	1	1	2	1	3	?
Pamirotheca	0	0	0	?	?	0	?	?	?	0	0	?	?	0	?	0	1	0	1	1	?	?	?	0
Parabifolium	?	0	0	3	0	0	?	?	?	?	?	?	?	0	3	0	?	0	1	1	?	?	?	0
Parathecidea hieroglyphica	0	?	?	3	0	?	?	?	?	0	?	?	?	0	2	0	1	0	1	1	?	?	?	0
Praelacazella wetherelli	2	0	0	4	0	0	1	2	0	0	1	1	0	0	3	0	1	0	1	1	2	0	5	?
Rioultina ornata	0	0	0	1	1	0	0	0	0	0	0	0	0	0	1	0	1	0	1	1	1	0	1	0
Thecidea radiata	0	0	0	3	0	0	1	3	3	1	1	1	1	0	2	0	1	0	0	0	1	1	3	0

Thecidella rustica	0	0	0	0	0	1	0	0	0	0	0	0	0	0	3	0	1	0	1	3	2	0	0	0
Thecidellina congregata	0	0	0	1	0	0	0	2	2	1	1	1	1	0	1	0	1	0	1	1	0	0	1	0
Thecidiopsis digitata	0	0	1	3	0	0	1	2	1	1	1	1	1	0	2	0	1	0	1	0	1	1	5	0
Thecospira haidingeri	0	0	0	0	0	0	0	0	0	0	0	0	0	0	0	1	1	1	1	1	1	0	0	0
Hungaritheca	0	0	0	?	?	?	?	?	?	?	?	?	?	0	1	1	1	0	1	1	?	?	?	?
Thecospirella	0	?	?	0	0	1	?	?	?	?	?	?	?	0	0	1	1	0	1	1	?	?	?	?
Vermiculothecidea vermicularis	1	0	0	1	0	0	0	?	?	?	?	?	?	0	3	0	1	0	1	1	?	?	?	0
Eolacazella longirostrea	?	?	?	3	1	1	0	3	3	0	0	0	0	0	3	0	1	0	1	1	2	1	?	0
Stentorina sagittata	0	0	0	5	0	1	?	0	0	0	0	?	?	0	1	0	1	0	1	1	?	?	?	0
Ancorellina	0	0	0	0	0	0	?	0	0	?	?	?	?	0	2	0	1	0	1	1	?	?	?	0

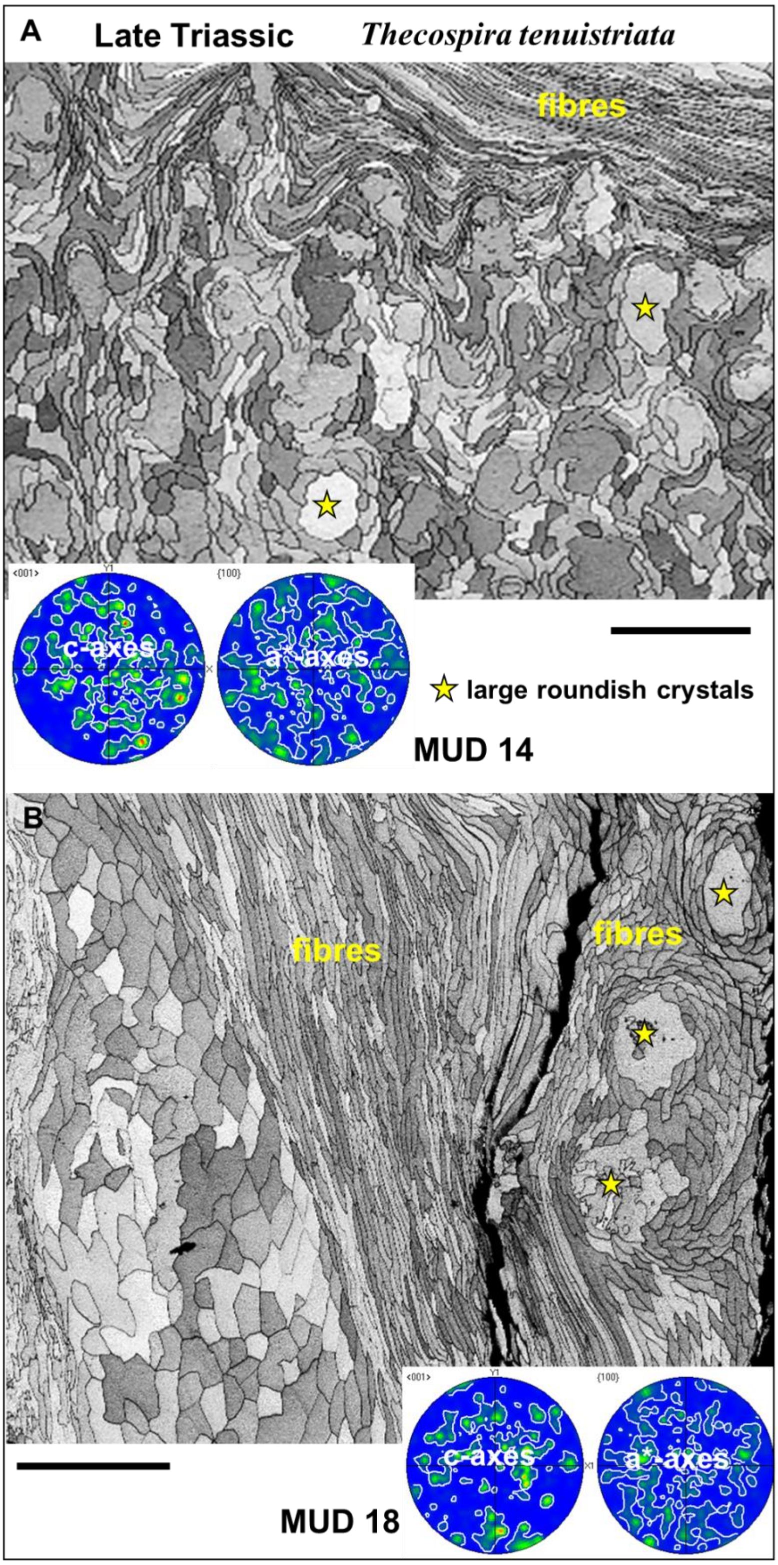

Figure S1. EBSD band contrast measurement image of the shell microstructure of the Triassic thecideide brachiopod *Thecospira tenuistriata* (MPU5804). The shell comprises small and large fibres and large rounded calcite units (yellow stars). Scale bars represent 100 µm.

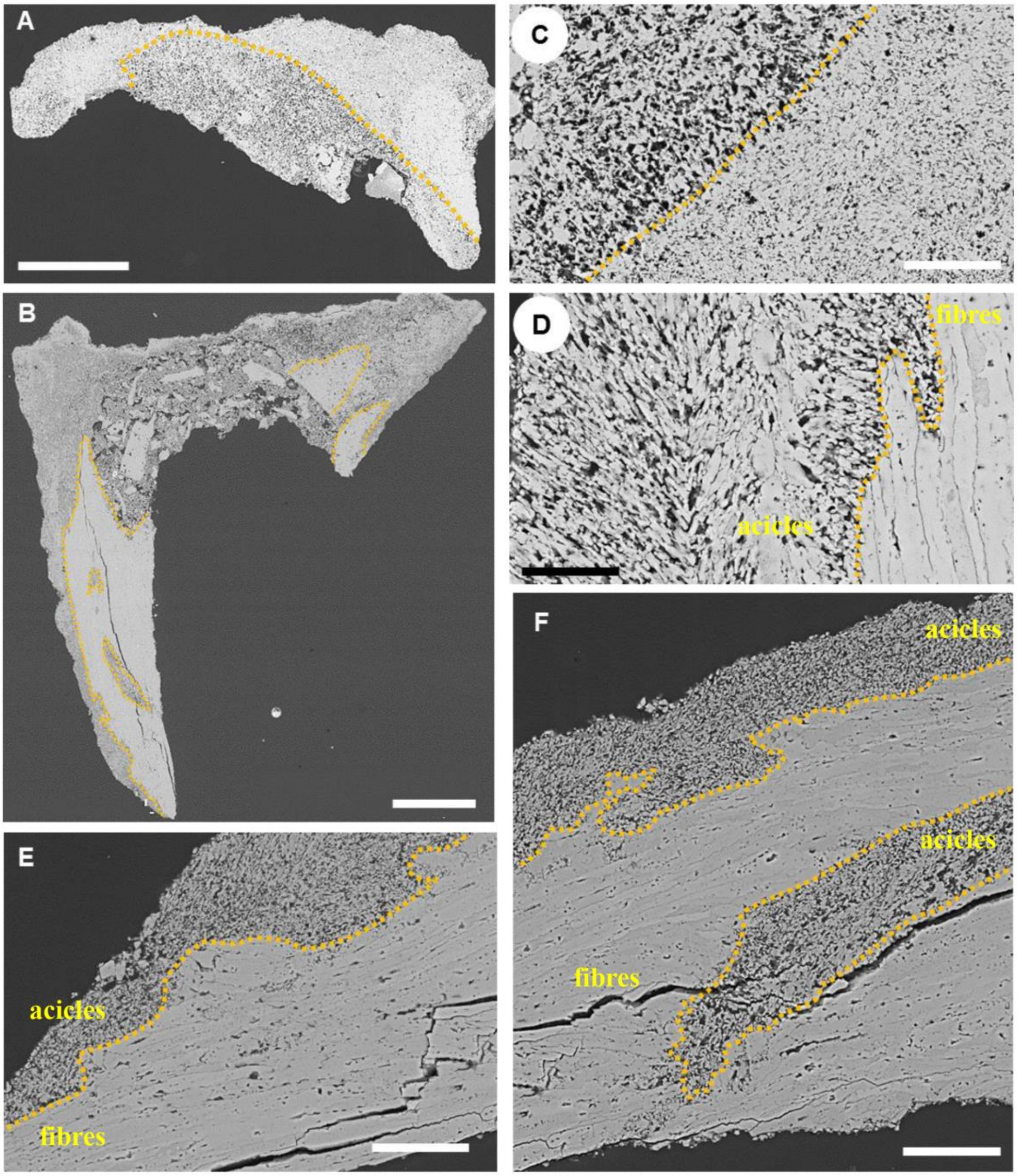

Figures S2. BSE images of shell layers of the Jurassic thecideide brachiopod *Neothecidella ulmensis* (LMU-NU01). Two microstructures form the shell of this species: acicles and fibres. Figures (A) and (B) show the distribution of the two microstructures in the dorsal (A) and ventral (B) valve, respectively. Acicular and fibrous shell portions are clearly distinguishable, see dashed yellow line. (C) is a detailed image of the acicles, in the left upper region the acicles are less dense in comparison with the right lower region. (D), (E) and (F) are detailed images of the contact between acicular and fibrous shell layers and the interdigitation of these. Scale bar represent 250 µm for A and B, 50 µm for C, E and F and 20 µm for D.

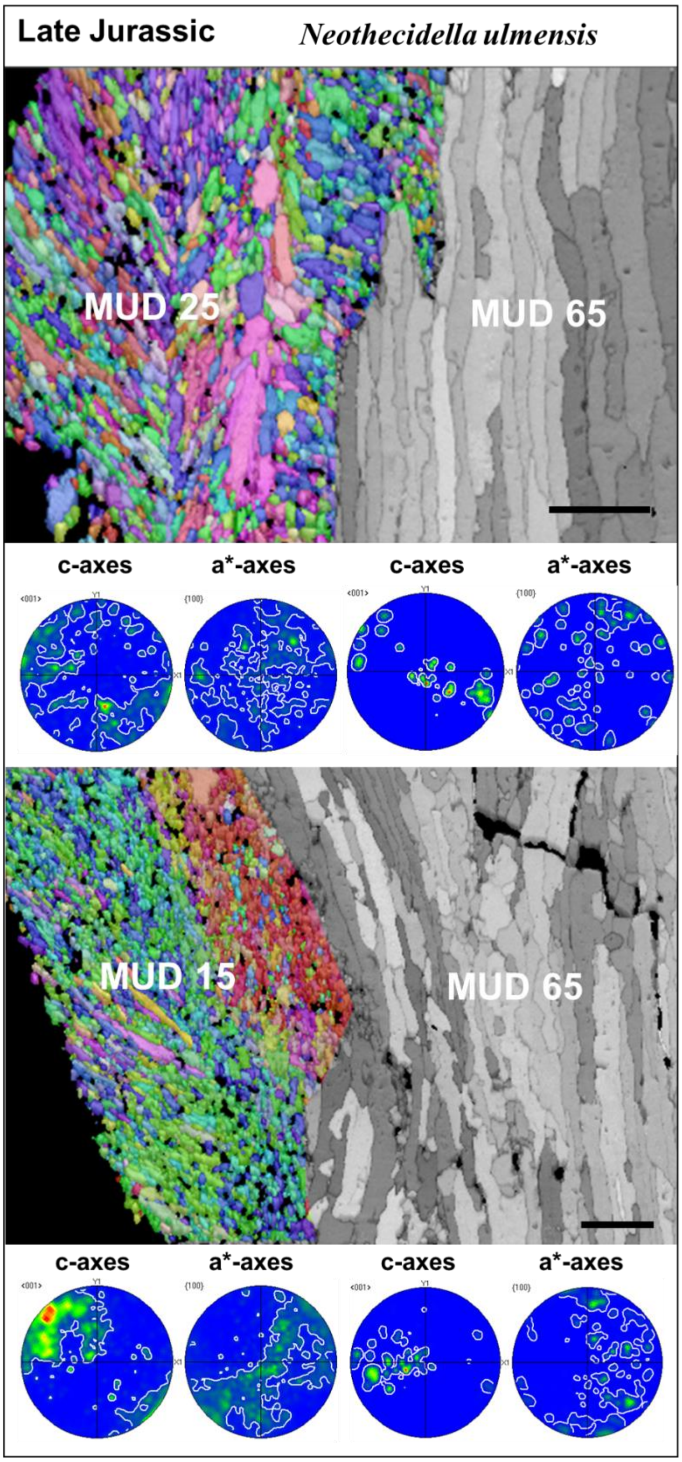

Figure S3. Calcite orientation (shown colour-coded) and band-contrast measurement images (shown grey-scaled) in the Jurassic thecideide brachiopod *Neothecidella ulmensis* (LMU-NU01) visualizing shell portions consisting of acicles (coloured) and of fibres (in grey), respectively. As the MUD values show co-orientation strength in the fibrous shell portion is higher (grey scaled), relative to acicular shell layers (coloured). Scale bars represent 20 µm.

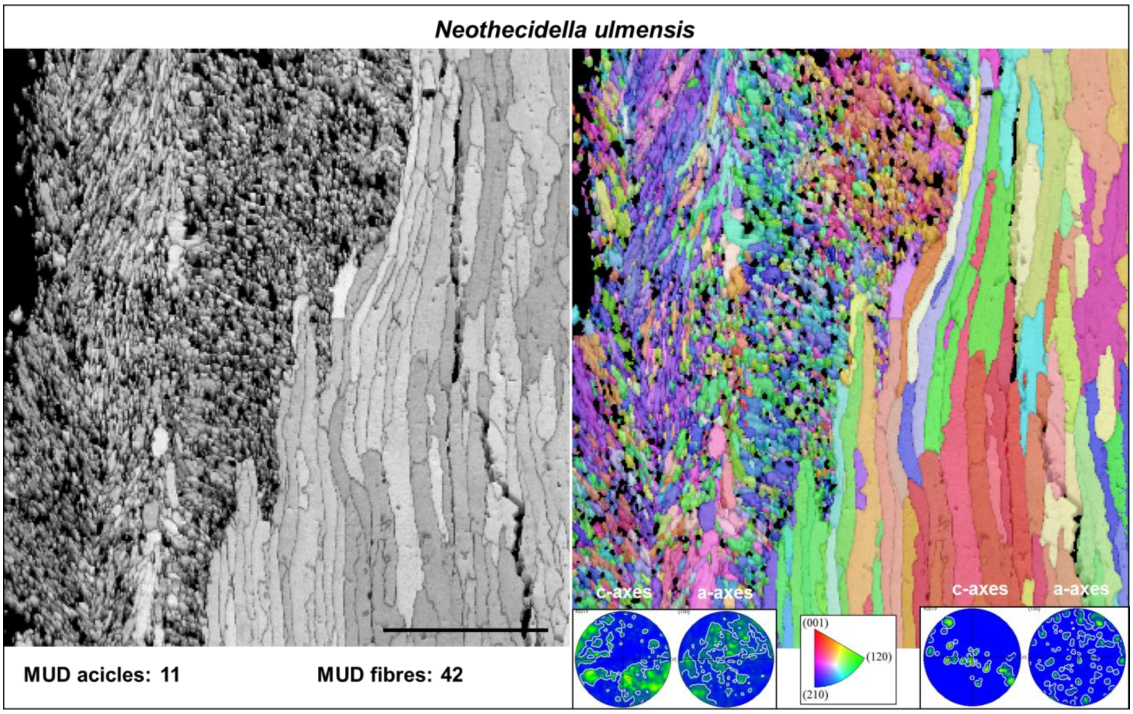

Figure S4. A further EBSD scan made on the shell of *Neothecidella ulmensis* (LMU-NU01) depicting calcite orientation (in color), band contrast measurement (grey-scaled) images, pole figures and giving MUD values for the acicular and fibrous shell portions. Scale bar represents 50 µm. The EBSD color code is given by the IPF triangle situated between the pole figures

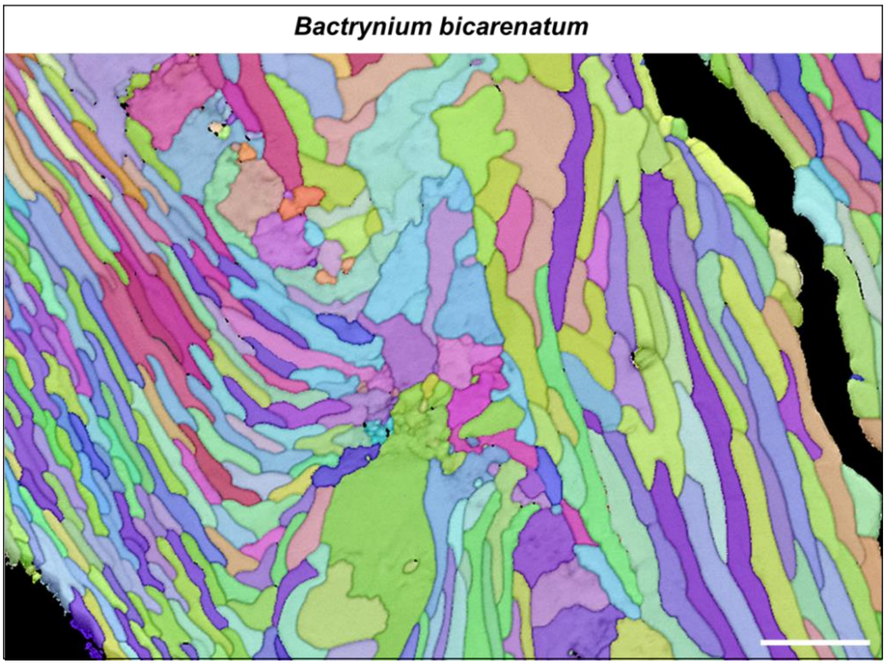

Figure S5. Orientation pattern of calcite shown colour-coded and derived from EBSD measurements for the shell of the Triassic thecideide brachiopod *B. bicarinatum* (E100-18-17). The EBSD colour code is given by the IPF triangle shown in Fig. S4. Scale bars represent 50 µm.

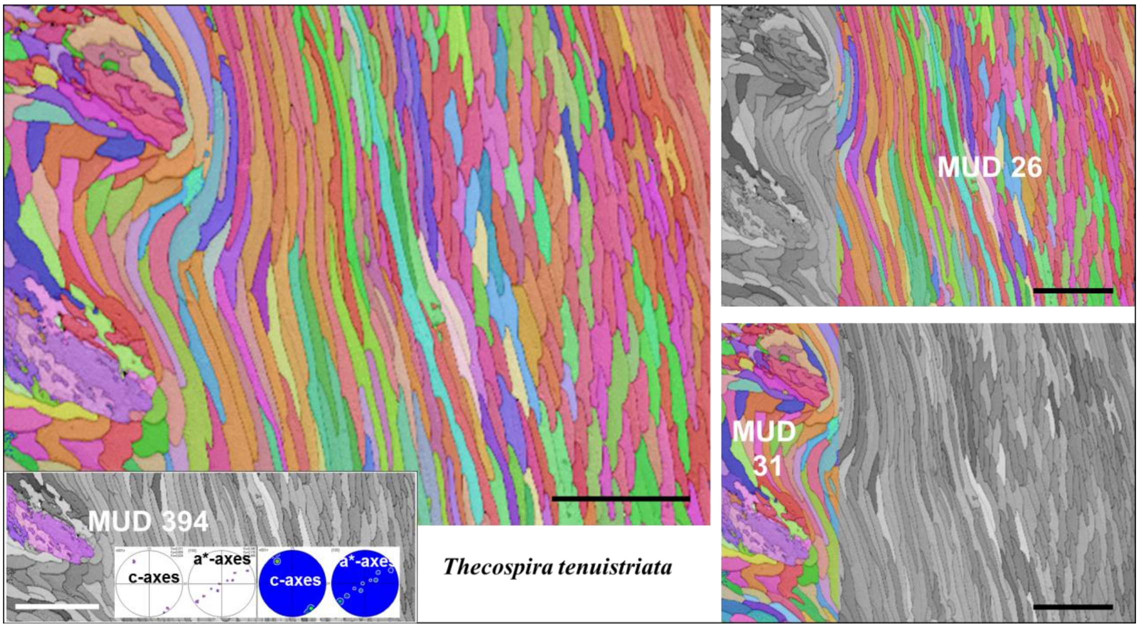

Figure S6. Orientation pattern of calcite shown colour-coded and derived from EBSD measurements for the shell of the Triassic thecideide brachiopod *Thecospira tenuistriata* (MPU5784-4). The MUD value for the array of fibres is 26; 31 for fibres and the large roundish calcite crystals and 394 for an individual large roundish calcite unit. The EBSD colour code is given by the IPF triangle shown in Fig. S4. Scale bars represent 50 µm.

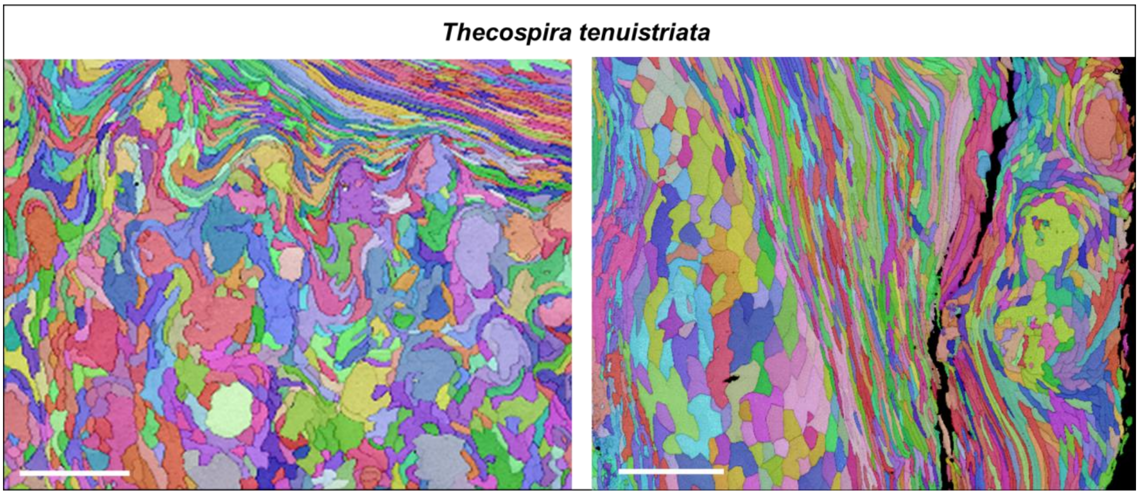

Figure S7. Orientation pattern of calcite shown colour-coded and derived from EBSD measurements for the shell of the Triassic thecideide brachiopod *T. tenuistriata* (MPU5804). The EBSD colour code is given by the IPF triangle shown in Fig. S4. Scale bars represent 100 µm.

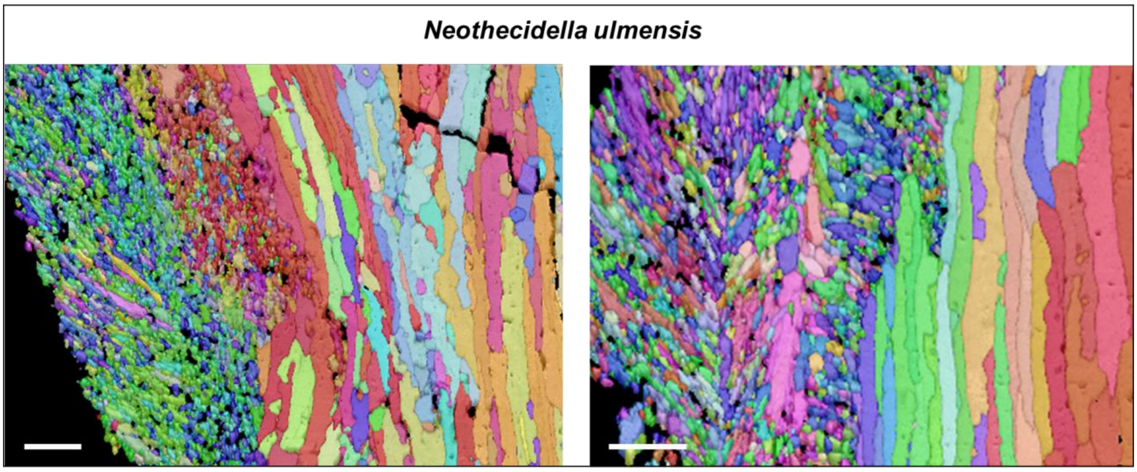

Figure S8. Orientation pattern of calcite shown colour-coded and derived from EBSD measurements for the shell of the Jurassic thecideide brachiopod *N. ulmensis* (LMU-NU01). The EBSD colour code is given by the IPF triangle shown in Fig. S4. Scale bars represent 20 µm.

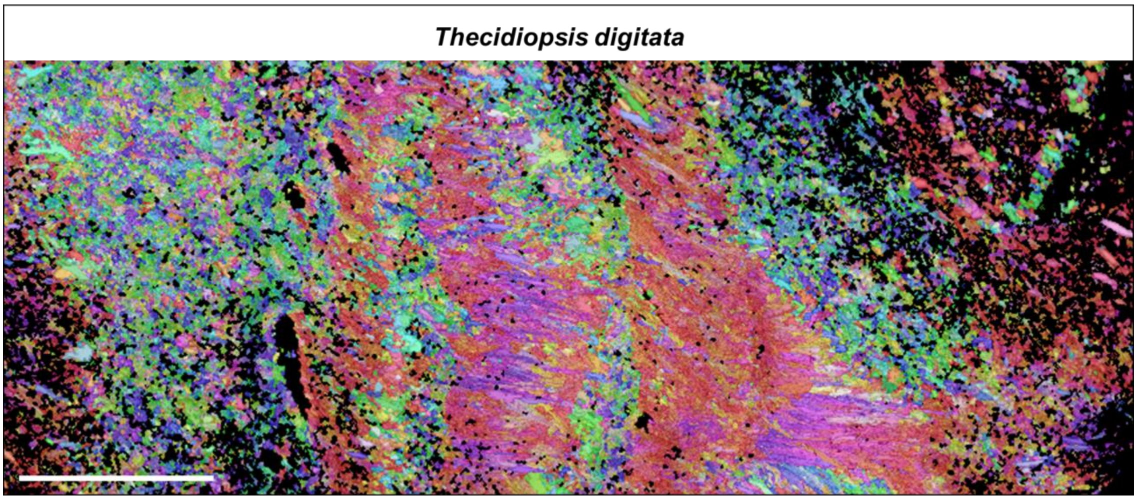

Figure S9. Orientation pattern of calcite shown colour-coded and derived from EBSD measurements for the shell of the Cretaceous thecideide brachiopod *T. digitata* (LMU-TD01). The EBSD colour code is given by the IPF triangle shown in Fig. S4. Scale bar represents 200 µm.

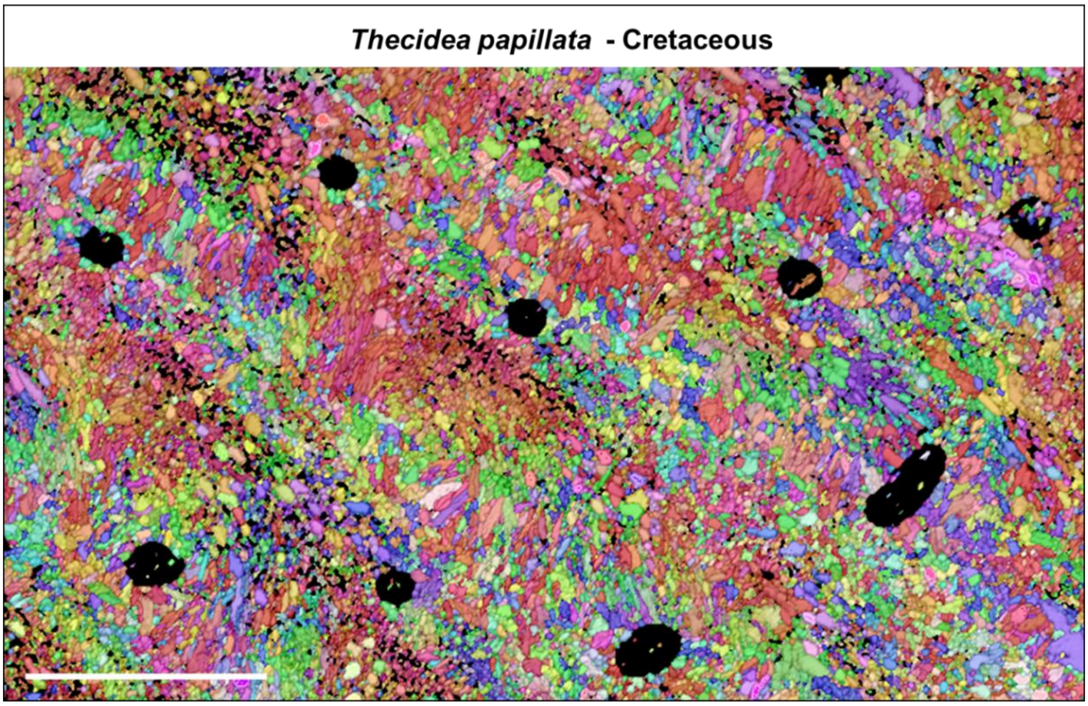

Figure S10. Orientation pattern of calcite shown colour-coded and derived from EBSD measurements for the shell of the Cretaceous thecideide brachiopod *T. papillata* (LMU-TPLC01). The EBSD colour code is given by the IPF triangle shown in Fig. S4. Scale bar represents 100 µm.

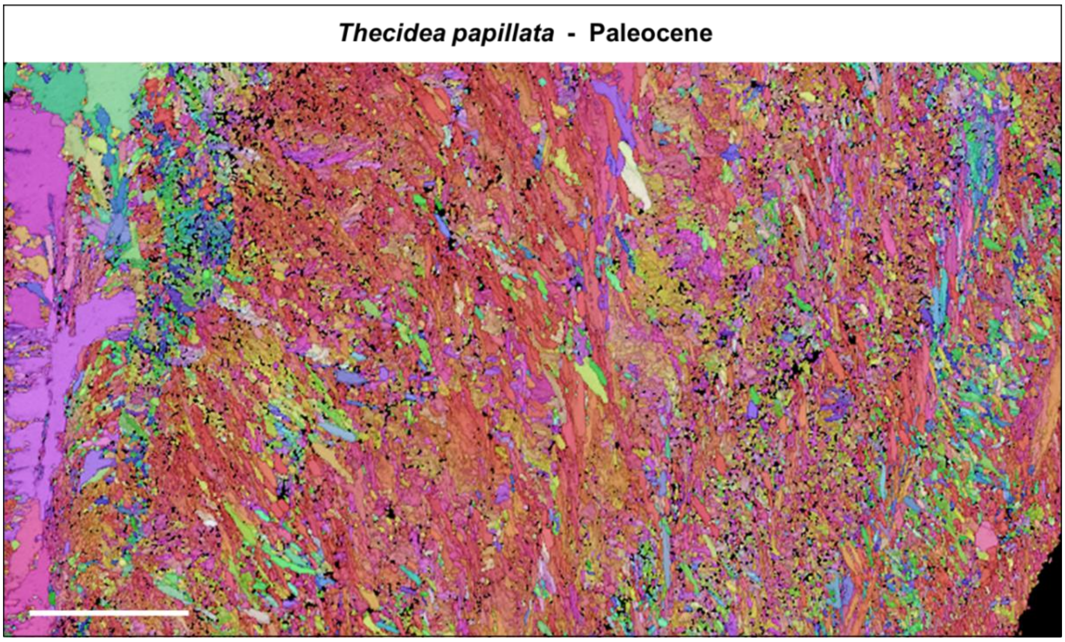

Figure S11. Orientation pattern of calcite shown colour-coded and derived from EBSD measurements for the shell of the Paleocene thecideide brachiopod *T. papillata* (LMU-TPP01). The EBSD colour code is given by the IPF triangle shown in Fig. S4. Scale bar represents 100 µm.

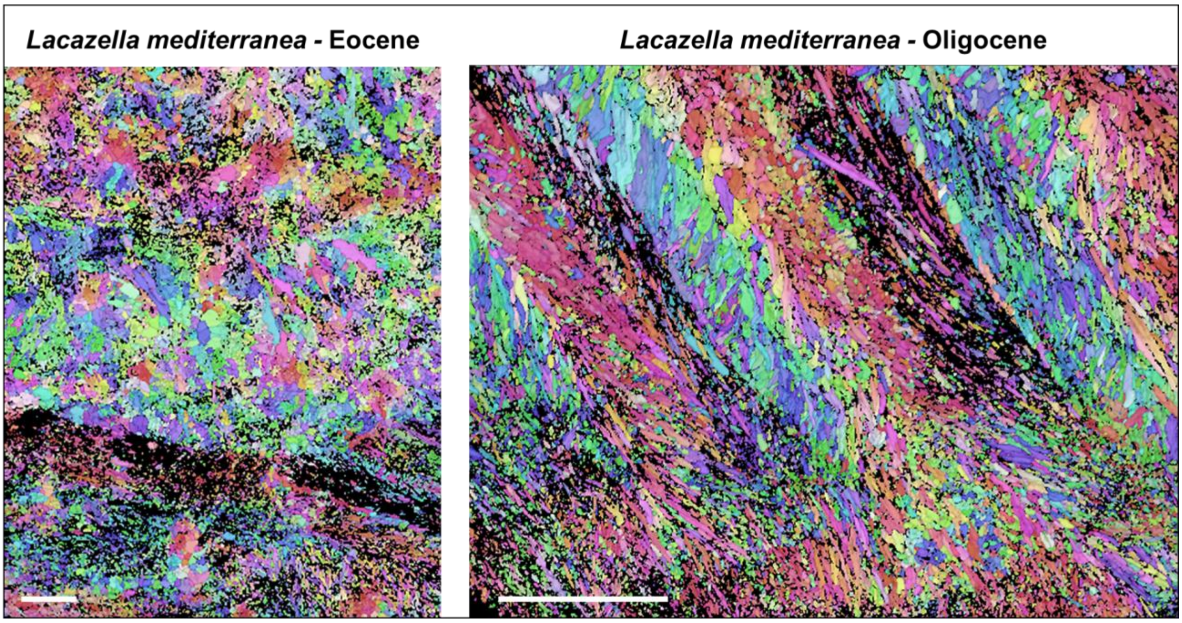

Figure S12. Orientation pattern of calcite shown colour-coded and derived from EBSD measurements for the shell of the Eocene and Oligocene thecideide brachiopod *L. mediterranea* (LMU-LME01 and LMU-LMO01 respectively). The EBSD colour code is given by the IPF triangle shown in Fig. S4. Scale bars represent 50 µm for the Eocene sample and 100 µm for Oligocene one.

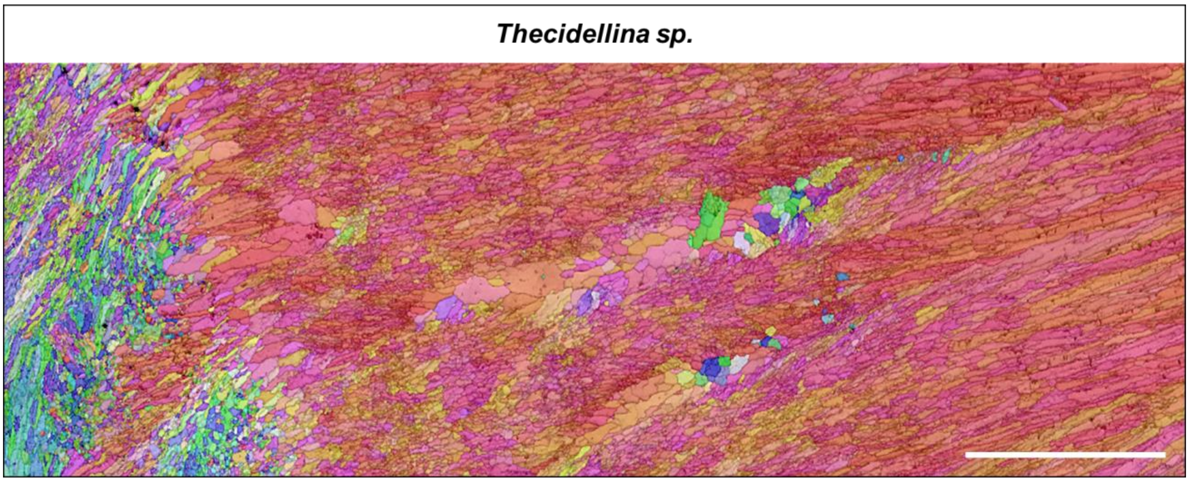

Figure S13. Orientation pattern of calcite shown colour-coded and derived from EBSD measurements for the shell of the Pleistocene thecideide brachiopod *Thecidellina* sp. (UF 325201). The EBSD colour code is given by the IPF triangle shown in Fig. S4. Scale bar represents 100 µm.

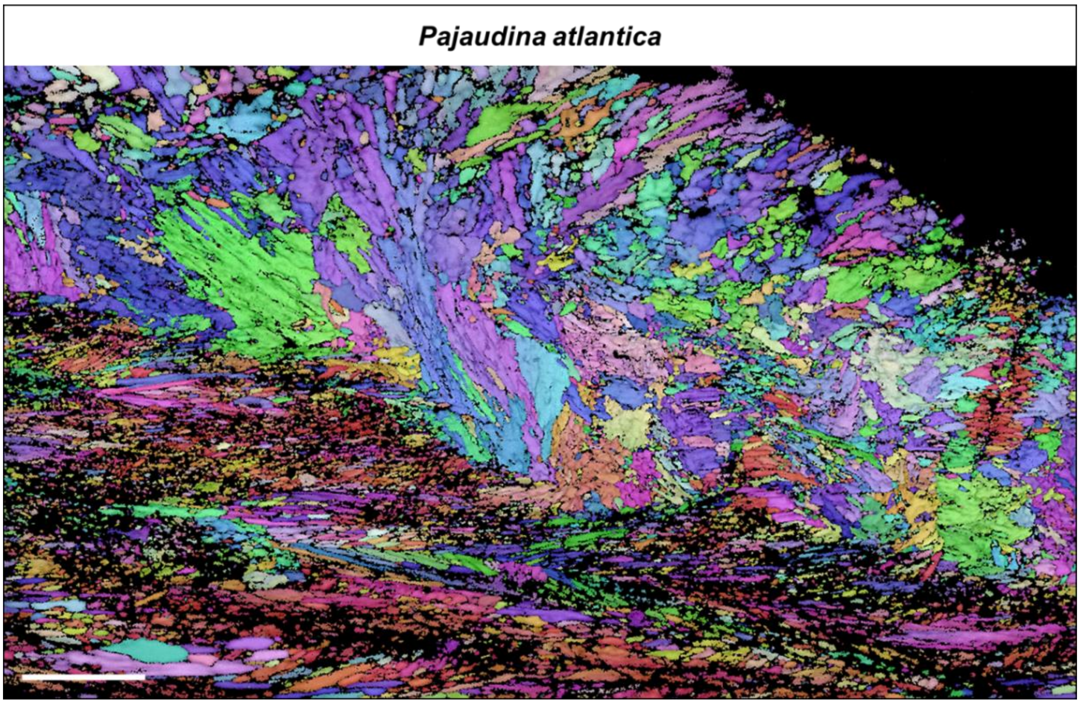

Figure S14. Orientation pattern of calcite shown colour-coded and derived from EBSD measurements for the shell of the Recent thecideide brachiopod *P. atlantica* (LMU-PA008). The EBSD colour code is given by the IPF triangle shown in Fig. S4. Scale bar represents 20 µm.

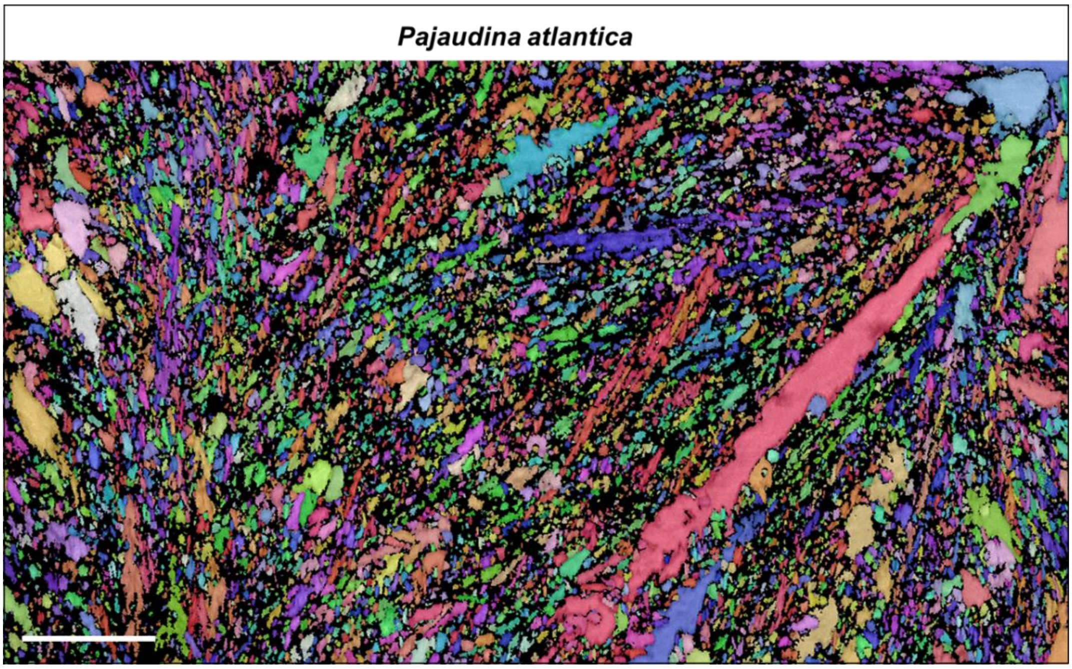

Figure S15. Orientation pattern of calcite shown colour-coded and derived from EBSD measurements for the shell of the Recent thecideide brachiopod *P. atlantica* (LMU-PA010). The EBSD colour code is given by the IPF triangle shown in Fig. S4. Scale bar represents 20 µm.

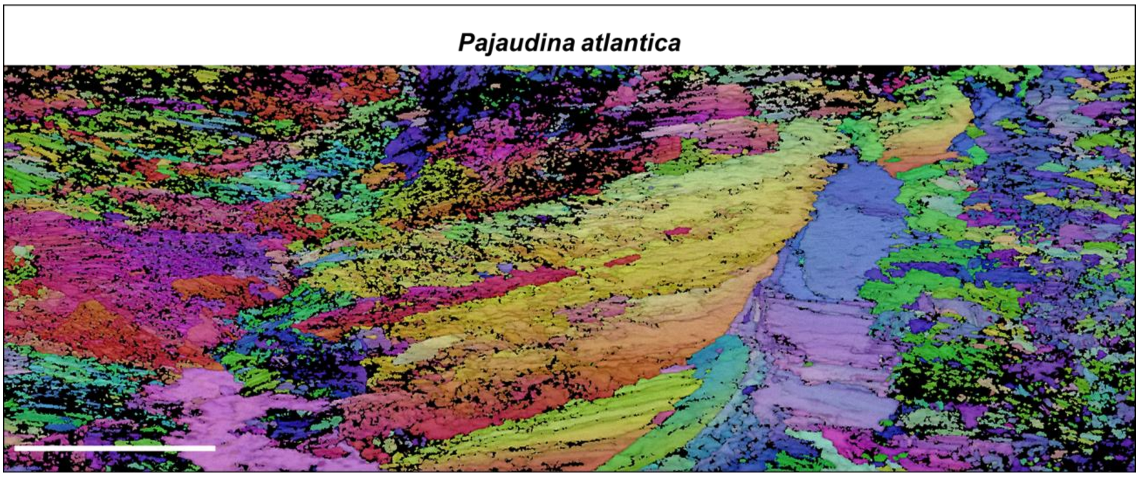

Figure S16. Orientation pattern of calcite shown colour-coded and derived from EBSD measurements for the shell of the Recent thecideide brachiopod *P. atlantica* (LMU-PA009). The EBSD colour code is given by the IPF triangle shown in Fig. S4. Scale bar represents 50 µm.

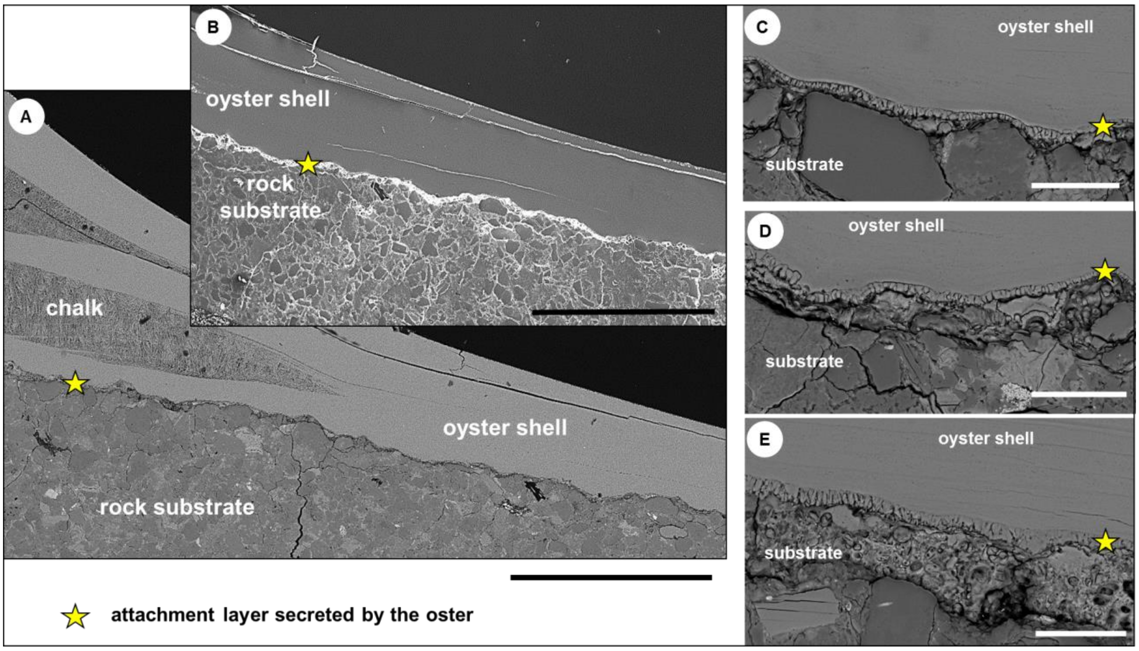

Figure S17. BSE images depicting the attachment of the shell of the oyster *Magallana gigas* onto the substrate. Attachment is made by a thin mineralized layer (yellow star in all images) secreted by the animal. The thickness of the attachment layer varies, depending on the roughness of the substrate. Scale bars represent 1mm for A-B and 50 µm for C-E.

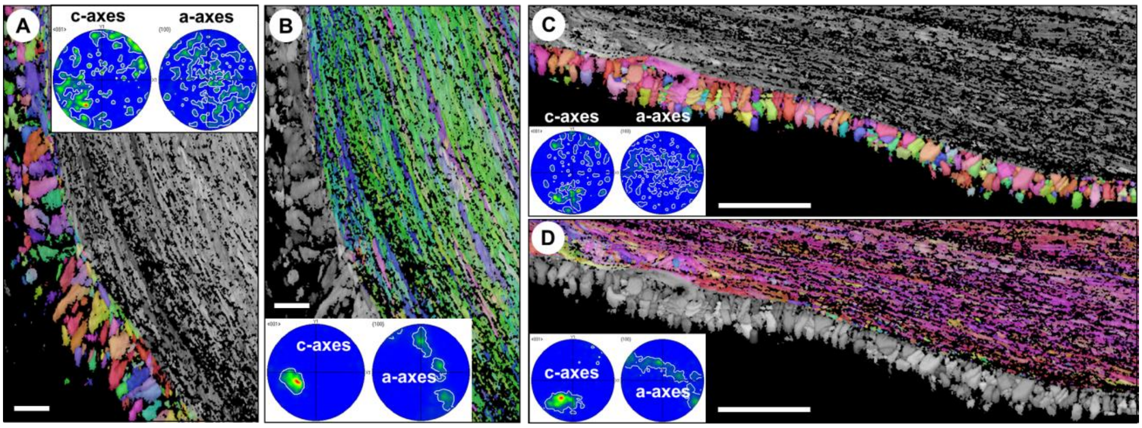

Figure S18. Orientation pattern of calcite shown with colour-coded EBSD maps and density distributions of associated pole figures for the attachment layer (A and C) and foliated calcite (B and D) of *Magallana gigas* shell. There is a significant difference in microstructure and texture: The strength of calcite co-orientation is low (MUD values 19, 21) within the attachment layer, while it is significantly higher (MUD values 38, 44) in the foliated calcite shell portion. Scale bars represent 10 µm for A-B and 20 µm for C-D.